JPE 17-1-17

https://doi.org/10.6113/JPE.2017.17.1.172
ISSN(Print): 1598-2092 / ISSN(Online): 2093-4718

A Fast-Transient Repetitive Control Strategy for Programmable Harmonic Current Source

Wanjun Lei†, Cheng Nie*, Mingfeng Chen*, Huajia Wang**, and Yue Wang*

†,*State Key Laboratory of Electrical Insulation and Power Equipment, Shaanxi Key Laboratory of Smart Grid, Xi'an Jiaotong University, Xi'an, China
**State Grid Shandong Electric Power Research Institute, Shandong, China

Abstract

The repetitive control (RC) strategy is widely used in AC power systems because of its high performance in tracking period signal and suppressing steady-state error. However, the dynamic response of RC is determined by the fundamental period delay T_0 existing in the internal model. In the current study, a ($nk \pm i$)-order harmonic RC structure is proposed to improve dynamic performance. The proposed structure has less data memory and can improve the tracking speed by $n/2$ times. T_0 proves the effectiveness of the ($nk \pm i$)-order RC strategy. The simulation and experiments of ($6k \pm 1$)-order and ($4k \pm 1$)-order RC strategy used in the voltage source inverter is conducted in this study to control the harmonic current source, which shows the validity and advantages of the proposed structure.

Key words: ($nk \pm i$)-order RC, Harmonic current source, Repetitive control (RC)

I. INTRODUCTION

The harmonic current source (HCS) is a kind of power electronic device that can precisely generate harmonic current. The HCS can provide specific quantitative measurement, which will easily verify the design scheme and directly improve the production technology level. Usually, the HCS is widely used in automatic testing and bench-top applications, such as avionics testing, IEC testing (standards IEC-61000-3-{2, 4} as example), shipboard testing, and power supply test applications.

In practical application, the working condition of electrical equipment is complicated. The output current of the HCS should follow instructions precisely to simulate the real working condition.

Numerous control schemes have been proposed for PWM inverters, such as PID control, PR control, deadbeat control, and sliding mode control [1]-[4], to achieve this requirement. However, these methods often fail to follow the harmonic current accurately to determine the intrinsic disadvantages of the controller or the parameter uncertainties. Repetitive control (RC), which is based on the internal model principle [5], can track any periodic signal and eliminate the steady-state tracking error. In [6] and [7], the digital form of the RC internal model is $1/(1 - Z^{-N})$, and the fundamental time delay is Z^{-N}, which means that the RC controller will not act in the first period when the instruction changes. Thus, the dynamic response of the RC controller is not satisfying and is suitable for fast-transient applications.

The internal time delay Z^{-N} determines the control speed of the RC. Many studies focused on decreasing the time delay Z^{-N} to improve the dynamic characteristics. In [8] and [9], a dual-mode RC structure, which composes even and odd harmonic RC internal models with the time delay $Z^{-N/2}$ and can improve error convergence speed by one time, was proposed. However, the parameter design is complex and needs accurate modeling. In [10], RC based on $T_0/6$ time delay under three synchronous reference frames (SRF), which can suppress the ($6n \pm 1$)-order harmonic current, was proposed. However, the performance decreases when unbalanced current exists in the system. In [11], the RC scheme takes $T_0/6$ as the time delay in the positive and negative SRF. The given control structure can be used in an unbalanced system at the cost of increasing the computational burden. When the PWM inverter uses LCL or

Manuscript received Jun. 8, 2016; accepted Nov. 17, 2016
Recommended for publication by Associate Editor Sung-Jin Choi.
†Corresponding Author: leiwanjun@mail.xjtu.edu.cn
Tel:+86-29-82667858, Fax:+86-29-82665223, Xi'an Jiaotong University
*State Key Laboratory of Electrical Insulation and Power Equipment, Shaanxi Key Laboratory of Smart Grid, China
**State Grid Shandong Electric Power Research Institute, China

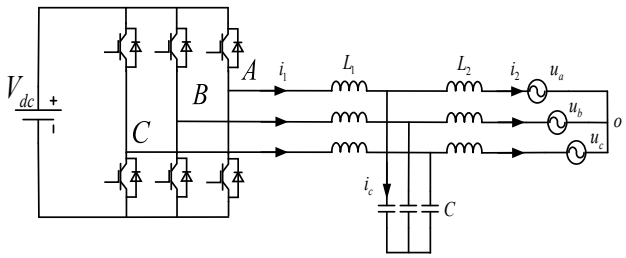

Fig. 1. Typical current control structure of the HSC with LCL filter.

other more complicated filters, the decoupling computation will increase significantly under the SRF axis.

In the current study, a fast-transient control strategy is proposed, which is a ($nk \pm i$)-order RC structure under the stationary axis. Compared with the conventional RC, the proposed strategy only needs less data memory and will increase the error convergence rate by n/2 times. Meanwhile, the controller is under the stationary axis, which can also eliminate the decoupling computation. The HCS with the proposed scheme will not only have fast-transient response but also low tracking error. The proposed structure is a unified RC form. Different n and i to set the ($nk \pm i$)-order RC internal model can be selected and used in the application, which only needs to eliminate specific order harmonics. The ($4k \pm 1$)-order and ($6k \pm 1$)-order RC are regarded as the main study object, and the parameter designing methods are obtained. Finally, simulations and experiments of the application of the HCS verify the effectiveness of the proposed ($nk \pm i$)-order RC scheme.

II. Model of HCS using ($nk \pm i$)-Order RC Strategy

A. Modeling of the Voltage Source Inverter (VSI) Using the LCL Filter

Fig. 1 shows that the HCS uses a three-phase VSI structure. The system consists of the DC bus source V_{DC}, IGBT inverter bridge, and grid-connected LCL filter (L_1 is the inverter inductor, L_2 is the grid inductor, and C is the filtering capacitor), in which u_s ($s = a, b, c$) is the AC grid source.

The damping part needs to be introduced to suppress the resonant peak of the LCL filter. Using a resistor, which is in parallel or in series with the capacitor C, is the easiest way to deal with this problem. However, the damping effect is proportional to the power loss on the resistor, implying that a good effect requires high power. Thus, the active resistor is proposed, and a feedback parameter is introduced in the control loop, which achieves the damping function acting as the power resistor but without power loss. Several methods are employed to achieve this. In the current study, the active resistor using the series resistor algorithm is chosen as the main method to suppress the resonant. The control diagram of the PWM

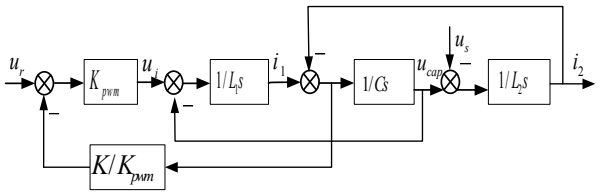

Fig. 2. Structure of active damping.

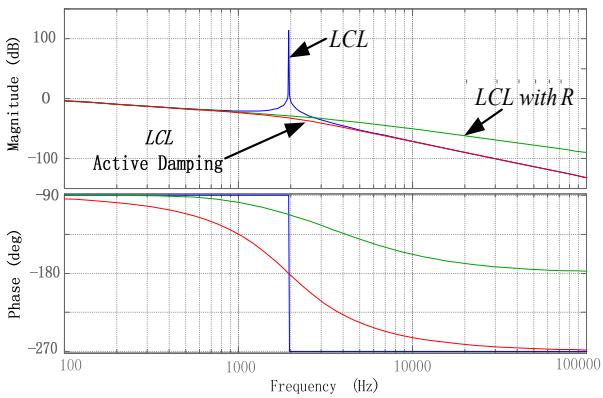

Fig. 3. Comparison of three LCL structures.

inverter with "equal-series resistor" [12] is shown in Fig. 2, where u_s is the source voltage, u_{cap} is the capacitor voltage, u_i is the voltage of the PWM inverter, and u_r is voltage reference.

The transfer function $G_p(s)$ in Fig. 2 can be written as:

$$G_p(s) = \frac{i_2}{u_r} = \frac{K_{pwm}}{\left(L_1L_2Cs^2 + KL_2Cs + (L_1 + L_2)\right)s}. \quad (1)$$

$G_p(s)$ can be regarded as the production of integral 1/s and a typical two-order system that introduces the resonant peak. According to control theory, when the damping coefficient of the two-order system ζ = 0.707, the resonant peak will disappear; the equation of coefficient K is expressed as [13]:

$$K = 2\xi\sqrt{\frac{L_1(L_1 + L_2)}{L_2C}}. \quad (2)$$

Fig. 3 shows the Bode plot of the LCL, LCL in series with the real resistor, and LCL with active damping, which shows that the last two methods have the ability to dampen the resonant peak. However, compared with the ideal LCL, the LCL with real resistor has higher gain at the high frequency range. The LCL with active damping exhibits a good performance and is almost the same as the ideal LCL, except for the resonant frequency. This finding indicates that the proposed control method will not influence the filtering effect.

B. ($nk \pm i$)-Order RC Internal Model

In practice, the harmonic current that exists in power electronic systems is always composed of the ($nk \pm i$)-order harmonic component. Thus, the special RC internal model, which is exactly suitable for ($nk \pm i$)-order harmonic elimination, is the easiest way to suppress the harmonic current. The diagram of the ($nk \pm i$)-order RC is shown in Fig. 4.

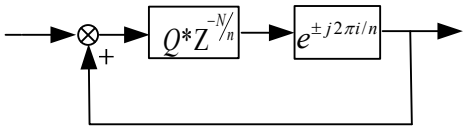

Fig. 4. The diagram of the ($nk \pm i$)-order RC internal model.

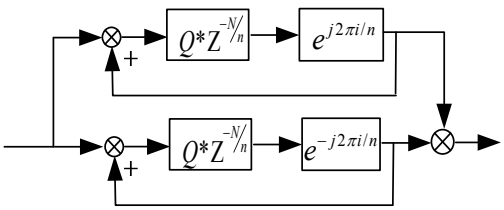

Fig. 5. ($nk \pm i$)-order RC internal model.

$$G_{RC}=\frac{Q\cdot z^{-N/n}\cdot e^{\pm j2\pi i/n}}{1-Q\cdot z^{-N/n}\cdot e^{\pm j2\pi i/n}} \tag{3}$$

In Fig. 4, the proposed RC internal model can follow the ($nk + i$)-order or ($nk - i$)-order harmonic current, and each part contains a time delay $Z^{-N/n}$, which means that this structure is n times faster than the conventional RC. A plural part $e^{\pm j2\pi i/n}$ must be introduced to move the resonant peak frequency from $nk\omega_0$ to ($nk \pm i$)ω_0 (where ω_0 is the fundamental frequency) to achieve the function mentioned in Eq. (3). However, achieving the plural part in a digital RC control system is impossible.

By adding two kinds of RC internal model, the parallel RC structure can be written as:

$$G_{RC}(z)=\frac{2\left(Q\cdot\cos 2\pi i/n\cdot z^{-N/n}-Q^2\cdot z^{-2N/n}\right)}{1-2Q\cdot\cos 2\pi i/n\cdot z^{-N/n}+Q^2\cdot z^{-2N/n}}. \tag{4}$$

The plural part in Eq. (3) is canceled for the conjugate plural part $e^{\pm j2\pi i/n}$, and the maximum time delay becomes $Z^{-2N/n}$. The poles of the parallel RC are located at ($nk \pm i$)ω_0 and introduce the resonant peak at those frequencies. According to the internal model principle, this kind of RC structure can achieve the zero-error tracking of ($nk \pm i$)ω_0 harmonics. Thus, the structure is called ($nk \pm i$)-order RC [14] (Fig. 5).

C. Plug-In ($nk \pm i$)-Order RC Structure

Fig. 6 shows the traditional "plug-in" RC structure, in which the ($nk \pm i$)-order RC structure is added to the forward path of the conventional control system. $G_p(z)$ is the controlled plant; $G_c(z)$ is the feedback controller; $G_{RC}(z)$ is the ($nk \pm i$)-order RC controller; R^* is the reference; $D(z)$ is disturbance signal; and $Y(z)$ is the output signal. This comprehensive structure has the advantages of the two controllers. If the feedback controller is designed properly to correct the plant (LCL filter) to a more stable and accurate system, then the parameter design of the ($nk \pm i$)-order RC would be easily obtained.

The stable parameter Q is used to make a good trade-off between accuracy and system stability, and the compensation part is used to cover for the phase delay and increases the high-frequency robustness.

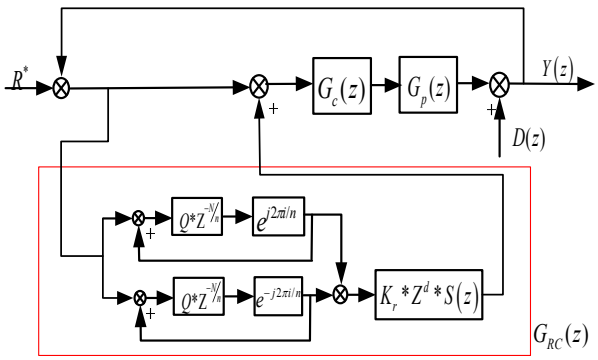

Fig. 6. Plug-in digital "$nk \pm i$" RC system.

The error transfer function of the "plug-in" ($nk \pm i$)-order RC can be expressed as:

$$\begin{aligned}e(z)&=\frac{1}{1+\left(G_{RC}+1\right)\cdot G_c\cdot G_p}\\&=\frac{1}{1+G_c\cdot G_p}\cdot\frac{1}{1+G_{RC}\cdot P(z)}\end{aligned}. \tag{5}$$

$P(z)$ in Eq. (6) is the closed-loop transfer function of conventional control, and the definition of the compensation part $G_f(z)$ is expressed in Eq. (7):

$$P(z)=\frac{G_c\cdot G_p}{1+G_c\cdot G_p}, \tag{6}$$

$$G_f(z)=K_r\cdot Z^d\cdot S(z). \tag{7}$$

Substituting Eqs. (4), (6), and (7) into Eq. (5), the following expression can be derived:

$$e(z)=\frac{1}{1+G_c\cdot G_p}\cdot\frac{1-2Q\cos\frac{2\pi i}{n}Z^{-\frac{N}{n}}+Q^2Z^{-\frac{2N}{n}}}{1-2Q\cos\frac{2\pi i}{n}Z^{-\frac{N}{n}}+Q^2Z^{-\frac{2N}{n}}+2\left(Q\cos\frac{2\pi i}{n}Z^{-\frac{N}{n}}-Q^2Z^{-\frac{2N}{n}}\right)\cdot G_f\cdot P(Z)}. \tag{8}$$

The conventional control is properly designed so that the system is stable. Guaranteeing the stability of the other part in Eq. (8) is essential. All of the roots of the characteristic equation should be in the unit circle. The equation is expressed as:

$$Z^{\frac{2N}{n}}=2Q\cos\frac{2\pi i}{n}Z^{\frac{N}{n}}\left(1-G_f*P(Z)\right)-Q^2\left(1-2*G_f*P(Z)\right). \tag{9}$$

III. Parameter Design of ($nk \pm i$)-Order RC

In many practical applications, particularly for the multiple-phase power systems, harmonic frequencies have specific characteristics. For example, for a single-phase power supply, ($4k \pm 1$)-order harmonics dominate the THD of its output currents/voltages; for a three-phase power supply with rectifier load, ($6k \pm 1$)-order harmonics dominate the THD; and

for n-phase HVDC transmission systems(n = 12, 18, 24, …), ($nk \pm 1$)-order harmonics mainly affect the system.

The harmonic current investigated in this study is in the ($6k \pm 1$)-order harmonic current, but is also included by the ($4k \pm 1$)-order RC. Thus, for the application of ($nk \pm i$)-order RC strategy in HCS, ($4k \pm 1$)-order and ($6k \pm 1$)-order RC are chosen as the study object.

A. (4k ± 1)-order RC

When n = 4 and i = 1, the internal model of "$nk \pm i$" RC is expressed as:

$$G_{RC(4k\pm1)}(z)=\frac{-2Q^2\cdot z^{-2N/n}}{1+Q^2\cdot z^{-2N/n}}. \tag{10}$$

Substituting Eq. (10) into Eq. (8), the new characteristic equation is expressed as:

$$Q^2\left(1-2*G_f*P(Z)\right)=-Z^{\frac{2N}{n}}. \tag{11}$$

This form is similar to the stability judgment criteria in [7], such that the conclusion of conventional RC stability judgment can also be applied in the ($4k \pm 1$)-order RC strategy. The stability judgment equation is expressed in Eq. (12). The system would be stable if the RC compensation is satisfied (Eq. (12)).

$$\left|1-2*G_f*P(Z)\right|<\frac{1}{Q^2} \tag{12}$$

Q is the limitation border in Eq. (12). The vector $1 - 2*G_f(z)*P(z)$ should be inside the circle whose radius is $1/Q^2$ over the entire frequency domain to make the $4k \pm 1$ RC system stable. The stability criteria can also be drawn to make the judgment more direct and easier, as shown in Fig. 7. Q is usually smaller than unit 1 to ensure a good trade-off between tracking accuracy and system robustness. Q can also be chosen as a zero-phase delay LPF to increase the stability margin and tracking accuracy, for example, $Q(z) = a_0z + a_1 + a_0z^{-1}$, with $a_0 + 2a_1 = 1$, $a_0 > 0$ and $a_1 > 0$.

The compensation part $G_f(z)$ can influence the stability and performance of RC. From Eq. (7), $G_f(z)$ is composed of three parts, namely, control gain K_r, phase delay compensation Z^d, and suppression filter $S(z)$. These parts should satisfy the following conditions:

(1) The range of K_r should be limited in the range $K_r \in [0,1]$.
(2) $S(z)$ is the low-pass filter whose corner frequency should be sufficiently large to contain the working frequency. $S(z)$ has a damping function to improve the high-frequency stability margin.
(3) Z^d should compensate the phase delay of $P(z)S(z)$ to ensure that it is close to a constant at low-medium frequency.

B. (6k ± 1)-order RC

When n = 6 and i = 1, the internal model of ($nk \pm i$)-order RC is expressed as:

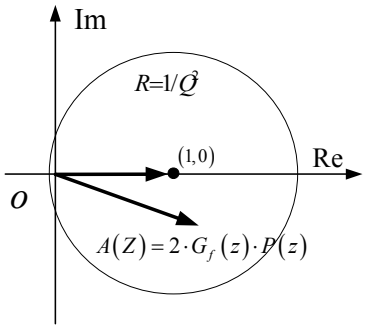

Fig. 7. Stability judgment of the ($4k \pm 1$)-order RC.

$$G_{RC(6k\pm1)}(z)=\frac{Q\cdot z^{-N/n}-2Q^2\cdot z^{-2N/n}}{1-Q\cdot z^{-N/n}+Q^2\cdot z^{-2N/n}}. \tag{14}$$

Substituting Eq. (14) into Eq. (9), the new characteristic equation is expressed as:

$$Z^{\frac{2N}{n}}=QZ^{\frac{N}{n}}\left(1-G_f*P(z)\right)-Q^2\left(1-2*G_f*P(z)\right). \tag{15}$$

Eq. (15) cannot use the criteria used in the ($4k \pm 1$)-order RC to evaluate stability, which is the only way is to prove whether all the poles are in the unit circle. However, the parameter design of the ($6k \pm 1$)-order RC is difficult and complicated. In [15], a method to evaluate the stability of the general ($nk \pm i$)-order RC system is proposed and still uses the $G_f(z)$ to compensate the feedback plant $P(z)$. The only difference is the form of $G_f(z)$ and $P(z)$.

Without loss of generality, $P(z)$ can be expressed as:

$$P(z)=\frac{z^{-d}B^+(z)B^-(z)}{A(z)}, \tag{16}$$

where all roots of $A(z) = 0$ are inside the unit circle, $B^+(z)$ is the cancelable parts of $B(z)$ and $B^-(z)$ is the noncancelable parts. $B^-(z)$ comprises roots on or outside the unit circle and undesirable roots that are in the unit circle and $B^+(z)$ comprises roots of $B(z)$ that are not in $B^-(z)$.

The compensation part $G_f(z)$ can be expressed as:

$$G_f(z)=\frac{z^dA(z)B^-\left(z^{-1}\right)}{B^+(z)b}, \tag{17}$$

where $b \geq \max |B - (e^{j\omega})|^2$ and z^d is used to compensate the phase delay of $P(z)$. $G_f(z)$ is regarded as an inverse function, and $G_f(z)P(z)$ can be written as:

$$G_f(z)P(z)=\frac{B^-\left(z^{-1}\right)B^-(z)}{b}\leq 1. \tag{18}$$

When $P(z)$ is stable and the range of the control gain $0 < K_r < 1$, the closed-loop system in Fig. 6 is asymptotically stable. In fact, $G_f(z)$ is used to ensure Eq. (18), but depends on the modeling accuracy and will be easily influenced when existing parameters drift.

In this study, the form in Eq. (7) is used, and the system will still be stable if the same conclusion is guaranteed as:

$$G_f(z)P(z)=K_r\cdot Z^d\cdot S(z)\cdot P(z)\leq 1. \tag{19}$$

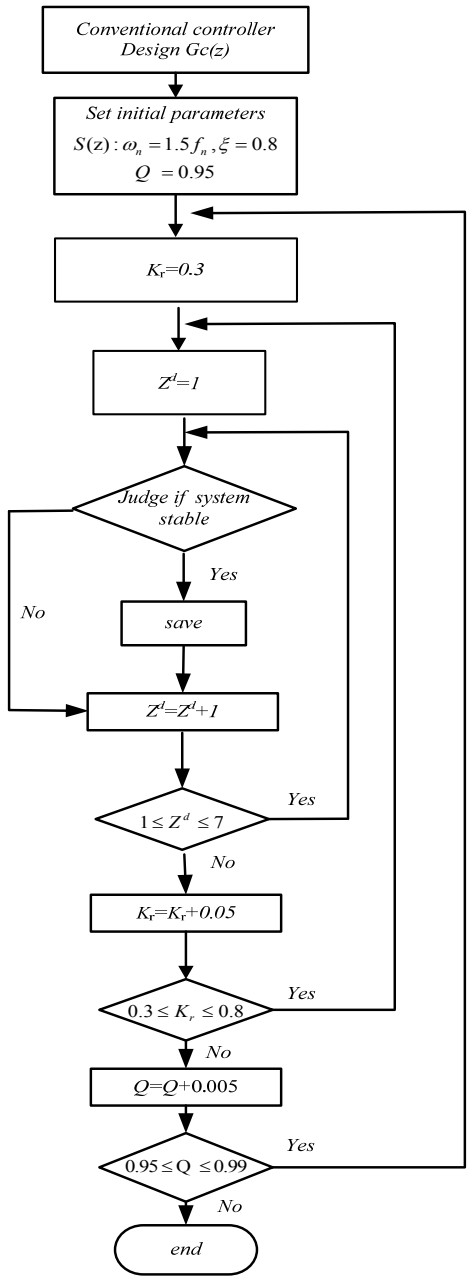

Fig. 8. Parameter design process of the $(6k \pm 1)$-order RC.

The range of the control gain is still $0 < K_r < 1$. Z^d compensates the phase delay of $S(z)P(z)$. If Z^d is properly selected, then $S(z)P(z)$ will be close to constant.

The values of Q, K_r, and Z^d are chosen through the trial and error method because the stability of the $(6k \pm 1)$-order RC could not be directly identified. The conventional controller $G_c(z)$ should first be designed. Then, Q and K_r should set the appropriate initial and final value limits and $S(z)$ can still use the form in Eq. (13). In a cycle loop, phase Z^d should be chosen to make the system stable. If the system is stable, then the parameter should be saved; if not, then it should be abandoned to jump out from the loop and set new data between the limits. In fact, Z^d must be an integer as the phase delay with an initial value of 1 and step length of 1. According to design experience, Z^d is designed from 1 to 7; K_r is designed from 0.3 to 0.8, which belongs to [0,1]; and Q is designed from 0.95 to 0.99. If the step length of Q or K_r is large, then the accuracy would be insufficient; if the step length of Q or K_r is small, then the computation period would be long. Given the variation range of K_r [0.3,0.8] and Q [0.95,0.99], 10% of the variation range is incremental change. Thus, given the precision and complexity of the entire test loop, the step lengths of Z^d, K_r, and Q are ensured, which are 1, 0.05, and 0.005, respectively. The design process is shown in Fig. 8. Finally, by comparing different qualified parameter simulations or experimental results, the most suitable parameters are chosen.

TABLE I
PARAMETERS OF THE HCS SYSTEM

HSC side inductor L_1	2 mH
Grid side inductor L_2	0.4 mH
Filter capacitor C	20 μF
DC bus voltage V_{DC}	200 V
Grid voltage (line RMS) u_s	60 V
Feed forward coefficient K	34

IV. SIMULATION AND EXPERIMENTAL VERIFICATION

In this study, the $(nk \pm i)$-order RC scheme is applied in the HCS. The parameters of the HCS are given in Table I. The simulation is conducted in the MATLAB simulation software, and the experiments are conducted on a DSP F2812 controlled platform. IGBT SEMIKRON SKM75GB128D is used as the inverter bridge. The simulation and experiments used phase A as the measure target to reduce the complexity and make the comparison clear. The study of the $(nk \pm i)$-order RC mainly focuses on two cases, namely, $(4k \pm 1)$-order and $(6k \pm 1)$-order RC. These cases have different control and sampling speeds. Thus, the control parameters should be analyzed separately.

A. $(4k \pm 1)$-order RC

In this case, the sampling and control frequency F_s is 10 kHz. At this frequency, the control parameters of the plug-in $(4k \pm 1)$-order RC are listed in Table II.

The parameters of the HSC are given in Table I. The controller $G_c(z)$ is designed by the conventional P method. Q, K_r, Z^d, and $S(z)$ are also given in Table II. Fig. 9 shows the locus plot of the corresponding vector $1 - 2*G_f(z)*P(z)$. The vector path is confined within the unity circle while $\omega \in [0,\pi/T_s]$, which means that the system is stable.

The internal model of the $(4k \pm 1)$-order RC contains a delay $Z^{-N/2}$, which means that the response of the $(4k \pm 1)$-order RC will be affected after the half fundamental period

TABLE II
CONTROL PARAMETERS OF THE $(4k \pm 1)$-ORDER RC

Sampling frequency	10 kHz
Proportion P	15
Stability parameter	0.95
RC control gain	0.6
Phase compensation	Z^5
Second-order LPF $S(z)$	$\frac{0.2799z^{-1}+0.1789z^{-2}}{1-0.8085z^{-1}+0.2673z^{-2}}$

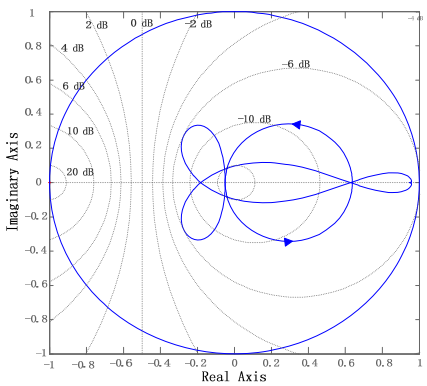

Fig. 9. Locus plot of the stability judgment of the $(4k \pm 1)$-order RC.

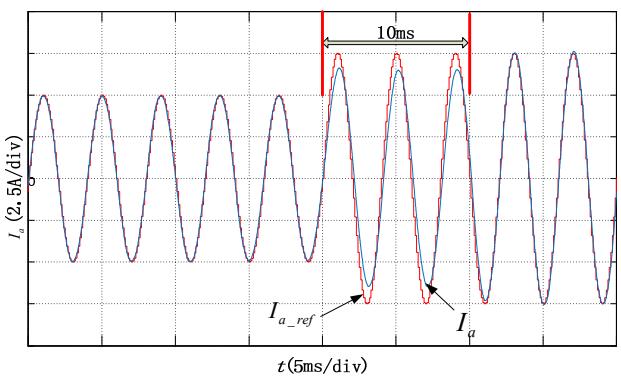

Fig. 10. Dynamic response of the $(4k \pm 1)$-order RC.

(approximately 10 ms). The fifth harmonic current is used as an example to conduct the simulations and experiments by suddenly changing the fifth harmonic current reference, which is shown in Figs. 10 and 11, to prove the dynamic response of this control scheme. Fig. 10 shows the simulation result. After the 10 ms time delay, the $(4k \pm 1)$-order RC begins and the output current will follow the instruction. Figs. 11(a) and 11(b) show the experimental results of instruction changes when the current error converges after 10 ms. This result is compatible with the result of the simulation.

The $(4k \pm 1)$-order RC HCS needs to follow the current with many harmonic orders when verifying its steady-state tracking effects. The harmonic instruction is shown in Table III. The output current and its tracking error are shown in Fig. 12. In the simulations and experiments, the current can follow the instruction precisely and the tracking error is suppressed

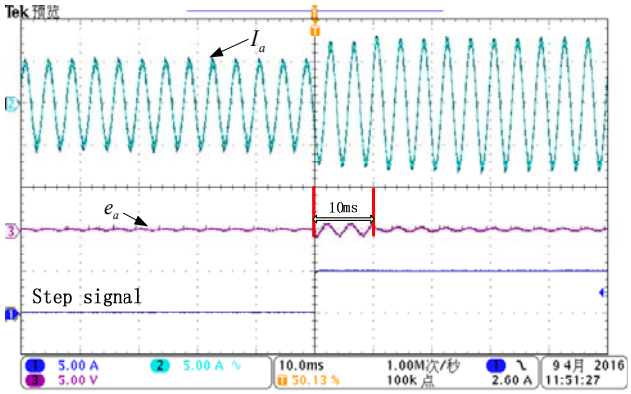

(a) Increasing instruction.

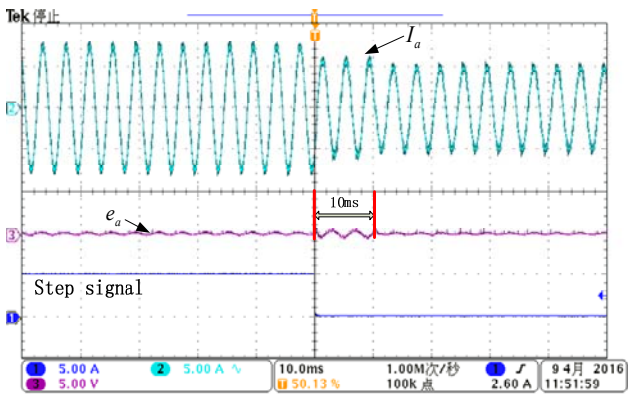

(b) Decreasing instruction.

Fig. 11. Dynamic response of the $(4k \pm 1)$-order RC.

TABLE III
HARMONIC CURRENT INSTRUCTION

Harmonic order (th)	Value (A)
5	2.5
7	2
11	1.5
13	1
17	0.5
19	0.25

close to zero. Quantitative analysis of the tracking error of each order harmonic component is also given in Fig. 13. The tracking error increases with the order of the harmonic. The highest order 19th is limited in 6%. Thus, the introduction of the $(4k \pm 1)$-order RC scheme improves the control speed without losing tracking error.

B. $(6k \pm 1)$-order RC

In this case, the sampling and control frequency F_s is chosen as 15 kHz. As analyzed previously, $G_f(z) = K_r Z^d S(z)$ of the $(6k \pm 1)$-order RC is designed using the trial and error method. The control parameters of the plug-in $(6k \pm 1)$-order RC are listed in Table IV.

The internal model of the $(6k \pm 1)$-order RC contains a delay $Z^{-N/3}$, which means that the response of the $(6k \pm$

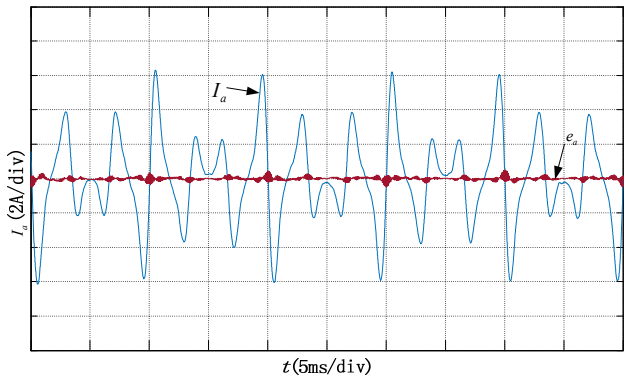

(a) Simulation verification.

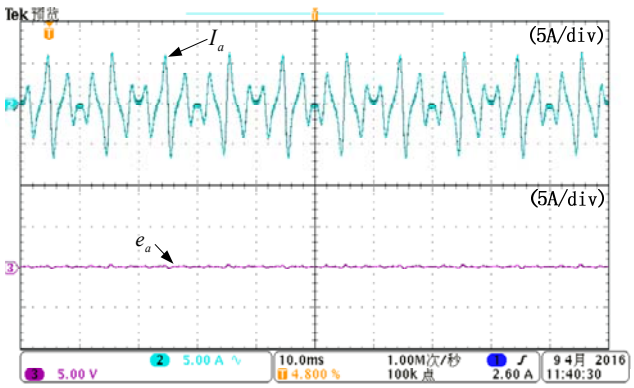

(b) Experiment verification.

Fig. 12. Output current and its tracking error of the $(4k \pm 1)$-order RC.

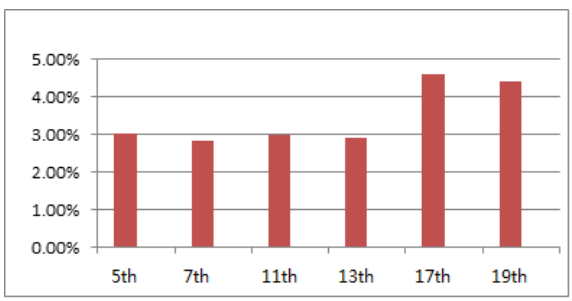

Fig. 13. Quantitative analysis of the tracking error percentage of the experiments.

TABLE IV
CONTROL PARAMETERS OF THE $(6k \pm 1)$-ORDER RC

Sampling frequency	15 kHz
Proportion P	15
Stability parameter	0.98
RC control gain	0.55
Phase compensation	Z^7
Second-order LPF $S(z)$	$\dfrac{0.1457z^{-1}+0.1084z^{-2}}{1-1.161z^{-1}+0.4149z^{-2}}$

1)-order RC will affect one third of the fundamental period (approximately 6.7 ms). The fifth harmonic current is chosen in the simulation and experiment by suddenly changing fifth harmonic current reference to prove its dynamic response.

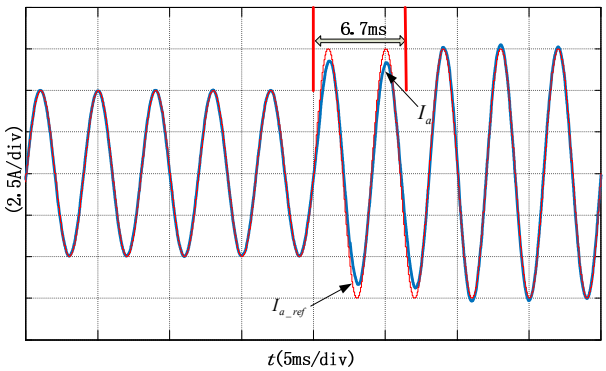

Fig. 14. Dynamic response of the $(6k \pm 1)$-order RC.

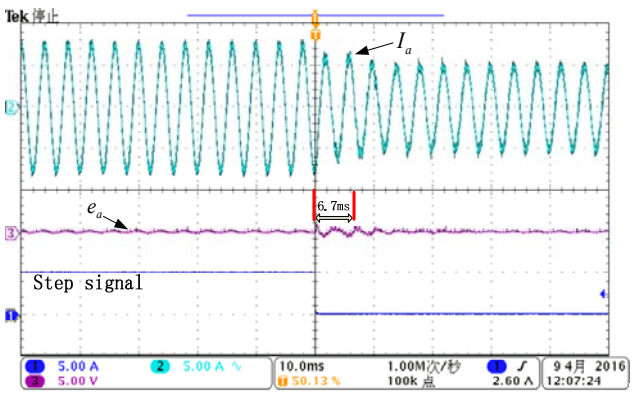

(a) Increasing instruction.

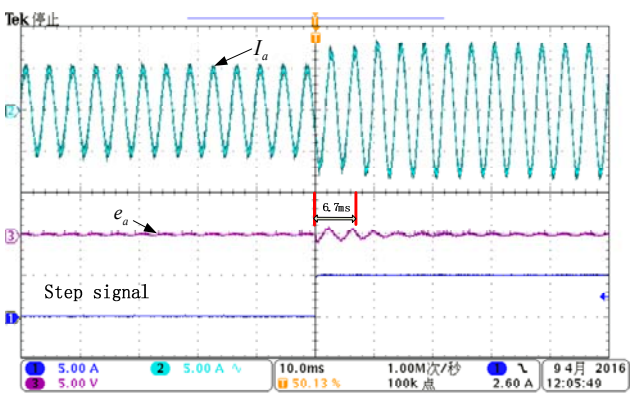

(b) Decreasing instruction.

Fig. 15. Experiments of the dynamic response of the $(6k \pm 1)$-order RC.

The simulation result is shown in Fig. 14. After approximately 6.7 ms time delay, the output current begins to follow the instruction. Figs. 15(a) and 15(b) show the experimental result of instruction changes, wherein errors begins to converge. Although it cannot follow the instruction in one control period for the error of modeling, the time delay is still compatible with the analysis. Thus, this controller can improve the dynamic response by three times compared with the conventional RC.

The harmonic instruction shown in Table III is used to verify the steady-state tracking effects of the $(6k \pm 1)$-order RC. The output current and its tracking error are shown in

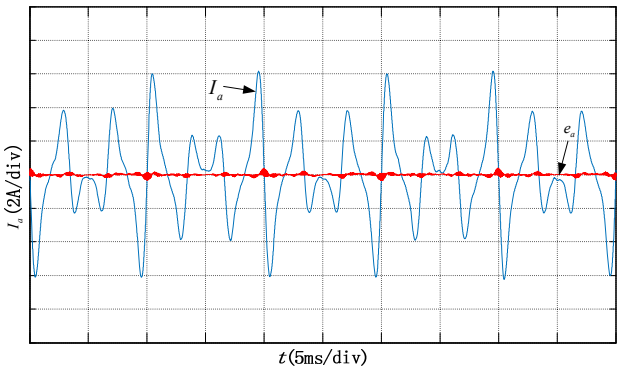

(a) Simulation verification.

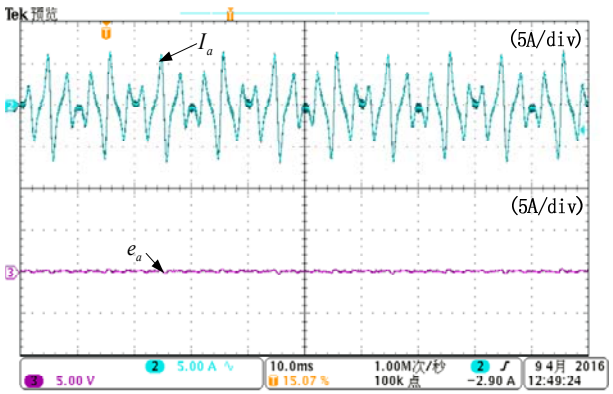

(b) Experiment verification.

Fig. 16. Output current and its tracking error of the ($6k \pm 1$)-order RC.

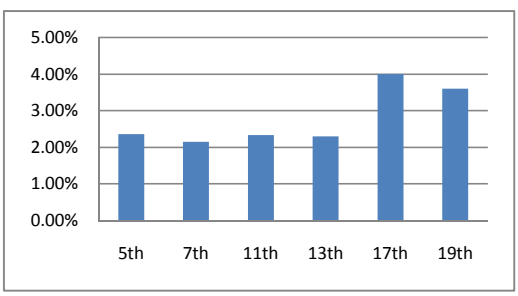

Fig. 17. Quantitative analysis of the tracking error percentage of the experiments.

Fig. 16. The results of the quantitative analysis of the tracking error of each order harmonic component are shown in Fig. 17. The tracking error in the simulation is still small, which means that the ($6k \pm 1$)-order RC still has high control precision.

V. Conclusions

This study proposes to use the ($nk \pm i$)-order RC strategy for the HCS. Compared with the conventional RC that has a fundamental time delay, the proposed strategy can improve the control speed by $n/2$ times without decreasing tracking accuracy. For a three-phase HCS system, simulations and experiments of the ($4k \pm 1$)-order and ($6k \pm 1$)-order RC were conducted to verify the effects of the ($nk \pm i$)-order RC. The proposed strategy is proven to have promising advantages over the conventional RC. This scheme is attractive for any three-phase system to achieve fast dynamic response and high tracking accuracy.

References

[1] Y. Han, L. Xu, M. M. Khan, C. Chen, G. Yao, and L.-D. Zhou, "Robust deadbeat control scheme for a hybrid APF with resetting filter and ADALINE-based harmonic estimation algorithm," *IEEE Trans. Ind. Electron.*, Vol. 58, No. 9, pp. 3893-3904, Sep. 2011.

[2] M. Angulo, D. A. Ruiz-Caballero, J. Lago, M. L. Heldwein, and S. A. Mussa, "Active power filter control strategy with implicit closedloopcurrent control and resonant controller," *IEEE Trans. Ind. Electron.*,Vol. 60, No. 7, pp. 2721-2730, Jul. 2013.

[3] L. R. Limongi, R. Bojoi, G. Griva, and A. Tenconi, "Digital current control schemes," *IEEE Ind. Electron. Mag.*, Vol. 3, No. 1, pp. 20-31, Mar. 2009.

[4] P. Mattavelli and F. P. Marafao, "Repetitive-based control for selective harmonic compensation in active power filters," *IEEE Trans. Ind. Electron.*, Vol. 51, No. 5, pp. 1018-1024, Oct. 2004.

[5] B. Francis and W. Wonham, "The internal model principle of control theory," *Automatica,* Vol. 12, No. 5, pp. 457-465, Sep. 1976.

[6] G. Escobar, A. Valdez, J. Leyva-Ramos, and P. Mattavelli, "Repetitive based controller for a UPS inverter to compensate unbalance and harmonic distortion," *IEEE Trans. Ind. Electron.*, Vol. 54, No.1, pp. 504-510, Feb. 2007.

[7] F. Botterón and H. Pinheiro, "A three-phase UPS that complies with the standard IEC 62040-3," *IEEE Trans. Ind. Electron.*, Vol. 54, No. 4,pp. 2120-2136, Aug. 2007.

[8] K. Zhou, D. Wang, B. Zhang, Y. Wang, J. A. Ferreira, and S. W. H. deHaan, "Dual-mode structure digital repetitive control," *Automatica,* Vol. 43, No. 3, pp. 546-554, Mar. 2007.

[9] K. Zhou, D.Wang, B. Zhang, and Y.Wang, "Plug-in dual-mode-structure repetitive controller for CVCF PWM inverters," *IEEE Trans. Ind. Electron.*, Vol. 56, No. 3, pp. 784-791, Mar. 2009.

[10] S. Jiang, D. Cao, Y. Li, J. Liu, and F. Z. Peng, "Low THD, fast-transient, and cost-effective synchronous-frame repetitive controller forthree-phase UPS inverters," *IEEE Trans. Power Electron.*, Vol. 27, No. 6, pp. 2994-3005, Jun. 2012

[11] C. Cosner, G. Anwar, and M. Tomizuka, "Plug in repetitive control for industrial robotic manipulators," in *Proc. IEEE Int. Conf. Robot. Autom.*, pp. 1970-1975, May 1990.

[12] W. Zhao and G. Chen, "Comparison of active and passive damping methods for application in high power active power filter with LCL filter," *Intemational Conference on Sustainable Power Generation and Supply*. *Nanjing: IEEE*, pp. 1-6, Dec. 2009.

[13] J. Dannehl, F. W. Fuchs, S. Hansen S, and P. B. Thogersen, "Investigation of active damping approaches for PI-based current control of grid-connected pulse width modulation converters with LCL filters," *IEEE Trans. Ind. Appl.,* Vol. 46, No. 4, pp. 1509-1517, Jul. 2010.

[14] W. Lu, K. Zhou, D. Wang, and M. Cheng, "A generic digital *nk* ± *m*-order harmonic repetitive control scheme for PWM converters," *IEEE Trans. Ind. Electron.*, Vol. 61, No. 3, pp. 1516-1526, Mar, 2014.
[15] W. Lu, K. Zhou, and D.Wang, "General parallel structure digital repetitive control," *Int. J. Control,* Vol. 86, No. 1, pp. 70-83, Jan. 2013.

Wanjun Lei received his B.S., M.S., and Ph.D. degrees in electrical engineering from the Xi'an Jiaotong University, Xi'an, China in 2000, 2004, and 2008, respectively. He is an assistant professor in the Department of Industry Automation, Power Electronics, and Renewable Energy Research Center at this university. He is a member of the China Power Supply Society and IEEE. His research interests include power electronics inverter, active power filter, reactive power compensation, and power quality control technique. W.J. Lei is with the State Key Laboratory of Electrical Insulation and Power Equipment, School of Electrical Engineering, Xi'an Jiaotong University, Xi'an, Shaanxi 710049, People's Republic of China.

Cheng Nie was born in 1985 in Hubei, China. He received his B.S. degree in electrical engineering from Hunan University, Changsha, China in 2008 and M.S. degree in electrical engineering from Xi'an Jiaotong University, Xi'an, China in 2013. He is currently working on his Ph.D. degree in the same university. His current research interests include microgrid, power quality, and analysis and control of multi-converter systems.

Mingfeng Chen was born in Zhejiang, China. He received his B.E. degree from Hangzhou Dianzi University, Hangzhou, China in 2014. He is currently working on his M.E. degree in Xi'an Jiaotong University. His research interests include power quality, active power filter, and reactive power compensation.

Huajia Wang was born in Shandong, China. He received his B.E. degree from Xidian University, Xi'an, China in 2013 and M.E. degree from Xi'an Jiaotong University, Xi'an, China in 2016. He is currently working as an assistant engineer in the State Grid Shandong Electric Power Research Institute. His research interests include power quality, active power filter, and reactive power compensation.

Yue Wang received his B.S. degree from Xi'an Jiaotong University, Xi'an, China in 1994, M.S. degree from Beijing Jiaotong University, Beijing, China in 2000, and Ph.D. degree from Xi'an Jiaotong University in 2004. He is currently a Professor at Xi'an Jiaotong University. His current research interests include active power filters, wind power generation, motor drives, multilevel converters, and VSC-HVDC.